Supersonic Jet Studies on the Photophysics of 4-Dimethylaminobenzonitrile (DMABN) and Related Compounds: on the Origin of the Anomalous Fluorescence of DMABN Clusters in a Supersonic Jet

Uwe Lommatzsch, Armin Gerlach, Christoph Lahmann, and Bernhard Brutschy*

Institut für Physikalische und Theoretische Chemie, Johann Wolfgang Goethe-Universität, D-60439 Frankfurt/M, Germany

Received: February 5, 1998; In Final Form: April 28, 1998

Dispersed fluorescence and resonant one-color, two-photon ionization spectra of clusters of six derivatives of 4-dimethylaminobenzonitrile (DMABN) expanded in a supersonic jet are reported. The studied clusters comprise molecules, that show dual fluorescence in solution and others, that do not. The experimental setup allows one to obtain information on the cluster size distribution in the pulsed supersonic expansion by time-of-flight mass spectrometry and to correlate the mass spectra with the species contributing to the dispersed fluorescence emission spectrum. Under jet-cooled conditions, no red-shifted fluorescence is observed for the bare chromophore of all compounds under study except 4-(dimethylamino)-3,5-dimethylbenzonitrile (TMCA). The formation of homogeneous clusters (dimers or small clusters) gives rise to an additional red-shifted emission band, which is attributed to the formation of excimers. The stabilization of the excimer arises from both exciton resonance and charge resonance interaction. The phenomenon of dual fluorescence of aminobenzonitriles in dilute polar solutions is usually attributed to an intramolecular charge transfer induced by a twist of the donor group around the bond between the donor and acceptor moiety [twisted intramolecular charge transfer (TICT)]. Because the red-shifted fluorescence is observed even for the molecules, that exhibit no dual fluorescence in solution, this mechanism cannot account for the observations made in this study. Fluorescence detection with a charge coupled device (CCD) camera in combination with an image intensifier shows the enrichment of the heavier clusters on the jet axis in a supersonic expansion. This angular dispersion of the species with different mass affords special techniques for correlating mass and fluorescence spectra.

Introduction

The dual luminescence of 4-dimethylaminobenzonitrile (DMABN) in polar solvents was discovered in 1959 by Lippert.[1] Since that time, various researchers have performed experiments on DMABN and derivatives, and various proposals have been given for this phenomenon.[2] In all mechanisms proposed, the underlying process is a charge transfer (CT). However, while some authors propose an intramolecular CT, others put forward an intermolecular CT.

The separation of charge upon photoexcitation of molecules is of basic importance in photosynthesis and plays a dominant role in many photochemical reactions. In the following report aminobenzonitriles may serve as model compounds for studying such CT processes. DMABN and some related compounds show two fluorescence emission bands (dual or anomalous fluorescence) if diluted in polar solvents. The high-energy band centered at $\lambda \sim 350$ nm is attributed to emission from the S_1 state (locally excited, LE or L_b state). A second red-shifted band at $\lambda \sim 420-500$ nm, the shift that is solvent dependent, is attributed to emission from a highly polar charge transfer state (L_a state).[2a] The CT is supported by the measurements of large dipole moments in the excited state.[3]

Several models explaining the phenomenon have been put forward rationalizing both static and dynamic studies in the solution phase and in supersonic jets. Apart from this experimental work, several contributions from theory tackled these problems based on quantum chemical calculations. The models differ fundamentally in the suggested structural relaxation of DMABN following the excitation of the S_1 state.

Grabowski and co-workers proposed the formation of a twisted intramolecular charge transfer (TICT) state, that develops out of the LE state.[4] As reflected in the acronym, this state is stabilized by a 90° twist of the dimethylamino group with respect to the aromatic ring. In this model, the twisting is coupled with an electron transfer from the dimethylamino group to the benzonitrile moiety leading to a drastic increase of dipole moment of the molecule. In the isolated molecule, the TICT and LE states are usually separated by a barrier. With increasing solvent polarity, this barrier is lowered and the stabilization of the TICT state is enhanced. These changes account for the occurrence of dual fluorescence mostly in polar solvents and the increase of the red shift of TICT emission with increasing solvent polarity. Because the emission from the TICT state takes place to a repulsive ground-state potential energy surface (PES), the emission band is structureless and red-shifted.[2a]

An alternative mechanism for the anomalous fluorescence was proposed by Varma et al.[5,6] based on an earlier suggestion by Chandross et al.[7] According to Varma, the occurrence of red-shifted fluorescence of DMABN also in a solution of nonpolar aromatic compounds is due to the formation of solute: solvent exciplexes with 1:1 and 1:2 stoichiometry. A sandwich structure for the exciplex was deduced from solvatochromic studies. Also, an increase of the pyramidalization of the dimethylamino group in the excited state was proposed.[8]

S1089-5639(98)01026-3 CCC: $15.00 © 1998 American Chemical Society
Published on Web 07/21/1998

Still another explanation has been given by Zachariasse et al.,[3,9,10] who put forward a solvent-induced pseudo-Jahn−Teller coupling as source for the anomalous fluorescence. According to this model, the conformational changes in the intramolecular CT (ICT) involve a planarization of the dimethylamino group and a deformation of the phenyl ring similar to radical anion formation of benzene. The efficiency of this process is governed by the magnitude of the energy gap between the nearby excited states S_1 and S_2.

Khalil et al.[11,12] rationalized the red-shifted fluorescence by assuming excimer fluorescence that was induced by the formation of dimers in the ground state. Evidence to contradict this excimer model was provided by Mataga et al.,[13] who found no dependence of the ratio of the intensities of normal and anomalous fluorescence on the concentration of the chromophore.

Recent theoretical calculations of varying quality supported the TICT mechanism.[14,15] From ab initio calculations, Sobolewski et al.[16] very recently proposed an in-plane bending of the nitrile group (rehybridization by ICT, RICT) as an alternative to the twisting of the dimethylamino group. In their calculation, an energy minimum in the excited-state potential energy surface for a conformation with a bond angle of ∼126° for the N−C−C_{phenyl} group was found. Experimental support for this hypothesis was given by Levy et al.[17] Gould et al.[18] questioned these theoretical results, finding in quantum chemical calculations a largely distorted and nonsymmetric structure with respect to the dimethylamino group of DMABN in the relaxed excited state.

None of these models is able to explain all experimental data completely. Quantum chemical studies of excited state dynamics refer mostly to the isolated molecule in the gas phase. Solvent effects can be approximated in theory only in a crude way. The theoretical modeling of experiments in solution often includes the simultaneous use of bulk quantities (e.g., dielectric constant) and molecular quantities (e.g., dipole moment) in a single equation for a microscopic description of a system consisting of a chromophore and a very small number of solvent molecules. These difficulties may be some of the reasons for the various mechanisms given for the dual fluorescence of these molecules in the literature.

Jet spectroscopy allows one to study in detail effects on a chromophore due to complexation with solvent molecules. The formation of ultra-cold van der Waals (vdW) clusters in a supersonic jet offers the opportunity to observe the influence of a more or less complex environment of solvent molecules on the photochemical behavior of the solute molecule. Jet studies on DMABN and related molecules have been recently reviewed by Itoh and Kajimoto.[19]

Complications in interpreting fluorescence spectra measured for a distribution of vdW clusters in a jet arise from the fact that all fluorophores contained in a beam contribute equally to the measured fluorescence spectra. Furthermore, it is difficult or nearly impossible to assign the size and the structure of the CT active clusters unambiguously. Although the size of a cluster can be more or less probed by mass spectrometry, its structure can be characterized only by sophisticated spectroscopic methods, such as rotationally resolved spectroscopy or rotational coherence spectroscopy. These methods have not been applied to DMABN until now.

The average size and structure of a cluster in a supersonic jet may be varied by changing the expansion conditions, such as the sample temperature or the mixing ratio of the expansion gases. These parameters are difficult to control, so different experimental setups often provide different results. Thus, in cluster studies, a certain process is often observed in different microscopic ensembles.

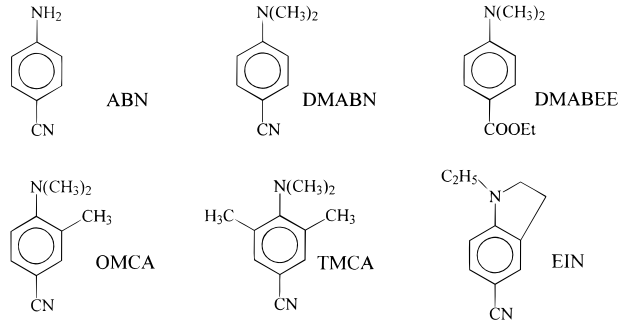

Figure 1. Compounds studied and their abbreviations used in the text.

In this work, an experimental setup is used to determine the cluster size distribution in the beam by time-of-flight (TOF) mass spectrometry, while the dispersed emission spectra is recorded nearly simultaneously. Ionization of the clusters is performed by resonant two-photon ionization via a resonant $S_1 \leftarrow S_0$ transition. This experimental setup greatly reduces the uncertainty of supersonic jet studies with regards to the species, which contribute to an emission spectrum, although this procedure may be limited by cluster fragmentation.

Here we report on the ion-yield curves, measured by resonance-enhanced one-color, two-photon ionization (R2PI), and on the dispersed fluorescence spectra of the bare monomer and of distributions of self-complexed clusters of 4-dimethylaminobenzonitrile (DMABN), 4-aminobenzonitrile (ABN), 4-(dimethylamino)-3-methylbenzonitrile (OMCA), 4-(dimethylamino)-3,5-dimethylbenzonitrile (TMCA), 1-ethyl-2,3-dihydroindole-5-carbonitrile (EIN) and 4-(dimethylamino)-benzoic acid ethyl ester (DMABEE). The molecules are depicted in Figure 1.

These molecules, which exhibit different ground-state geometries and photophysical properties were selected to get insight in the origin of the red-shifted fluorescence under jet-cooled conditions. For some of the molecules studied, anomalous fluorescence in a supersonic jet arising from homogeneous clusters has already been reported in the literature.[2c] However, the origin of this red-shifted fluorescence could not be identified unambiguously in all cases. In this study, we try to elucidate the origin of this dual fluorescence by comparing the photophysical behavior of this group of related but nevertheless (as will be seen) different molecules.

For ABN in the solution phase no dual fluorescence is reported in the literature, even in highly polar solvents.[3] In EIN the amino group is rigidly fixed in the plane of the phenyl ring. Therefore, the conformational flexibility (e.g., the twisting motion) of the amino group is extremely restricted. Also for EIN, no dual fluorescence is observed in solution.[20] In our cluster experiments, ABN and EIN serve as test compounds for which no red-shifted fluorescence is expected, at least if the TICT mechanism is the only one active for CT emission. The model proposed by Zachariasse et al.[3,9,10] also predicts the absence of anomalous fluorescence for these molecules.

OMCA and TMCA have a pretwisted conformation of the dimethylamino group in the ground state due to the additional methyl group(s) in ortho-position relative to the dimethylamino group. The conformations of OMCA and TMCA should therefore favor the formation of a TICT state. The inital excited state of DMABEE was proposed to directly (adiabatically) transform into the CT state, because of the stronger acceptor group.[21]

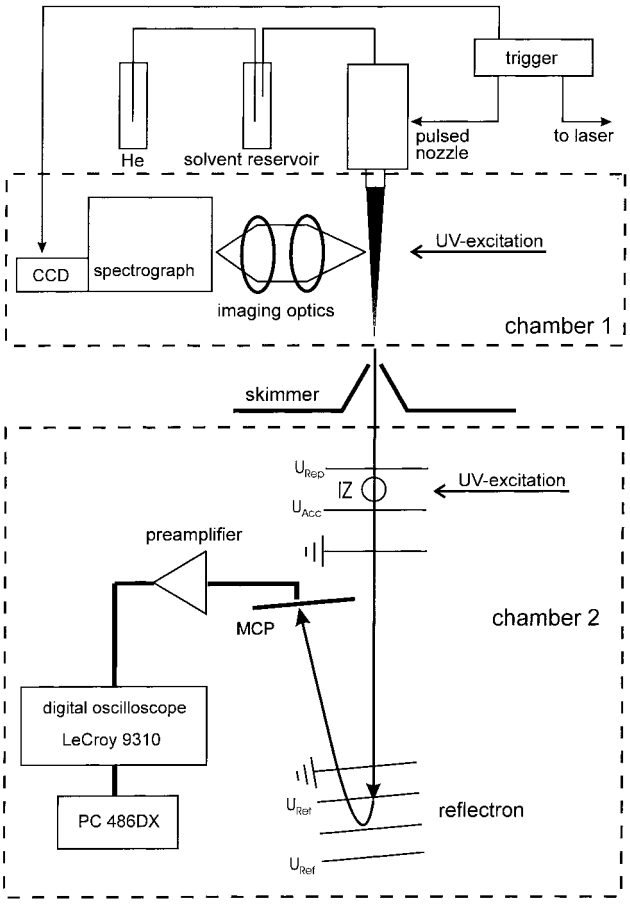

Figure 2. Schematic picture of the experimental setup. Each chamber is evacuated by a 1000 L/s turbo molecular pump (Turbovac 1000, Leybold-Heraeus) backed by a Roots blower (WKP 500, Balzers) and a rotary vane vacuum pump (DUO 60A, Balzers). The background pressure in the first and second chambers was, under operating conditions, typically 10^{-6} and 10^{-7} mbar, respectively. The skimmer separates chamber 1 from chamber 2. The ionization centrum is denoted by IZ, where the cations are accelerated up to 2.6 keV typically resulting in overall flight times of 20 μs.

A strongly red-shifted continuous fluorescence is also observed for many aromatic molecules in concentrated solutions. This red-shifted emission has been associated with the formation of a strongly bound dimeric species, which were denoted as excimers.

Experimental Section

A schematic picture of the experimental setup is shown in Figure 2. The vacuum system of the supersonic beam apparatus consists of two differentially pumped vacuum chambers connected via a 5.0-mm diameter skimmer. Chamber 1 houses the pulsed supersonic beam source and some optics to collect the emitted fluorescence after exciting the molecules in the beam by UV laser light. In chamber 2, the clusters are ionized by one-color resonant two-photon excitation using the same laser as for the fluorescence excitation and are subsequently mass analyzed in a home-built reflectron TOF mass spectrometer. The axis of the latter is coaxial to the beam axis. Ionization takes place in a two-stage parallel-plate ion source placed behind the skimmer. Generally, the laser intensity was kept $<10^6$ W/cm^2.

To measure R2PI spectra, the ion yield at a selected mass is recorded while scanning the wavelength of the exciting laser. The ions are amplified in a dual microchannel plate detector. The output of which is fed into a 300 MHz amplifier (Phillips, model 771) and digitized in a 300 MHz digital transient recorder (LeCroy 9310). The accumulated spectra are transferred to a PC via a general purpose interface bus (GPIB) interface.

Fluorescence is excited in chamber 1 at a distance of ~10 mm from the nozzle ($x/D = 20$, where x is the distance from the nozzle and D is the nozzle diameter) and is collected perpendicular to both the laser and molecular beam by a collection optic, consisting of a retro-reflecting mirror and a two-lens system. The emitted light is focused onto the entrance slit of a $f = 250$ cm spectrograph (Chromex 250IS). The spectrograph is equipped with toroidal mirrors for reducing image distortion in the focus plane and two gratings with 300 and 1200 lines/mm blazed at 400 and 330 nm, respectively. Usually, the spectra were recorded in first order. The typical slit width used was 80 μm. The dispersed fluorescence is imaged onto a charge coupled device (CCD) camera (Flame Star-III, LaVision) after its conversion by a photocathode and a time-gated intensification by a channel plate. The gate of the image intensifier has a time resolution of 5 ns and is used to suppress scattered laser excitation. Luminescence has been detected within 400 ns after laser excitation. The fluorescence detection system is controlled by a PC. Spectra were accumulated for 2−3 min. The size of the CCD detector (1024 × 256 pixel, pixel area 23 × 23 μm^2) allows one to simultaneously record a spectral range of ~200 nm (with the 300 lines/mm grating). Calibration was performed with the help of a mercury lamp (Oriel 6035) using the wavelengths suggested by Sansonetti et al.[22] The spectral resolution for the low dispersing grating is ~60 cm^{-1}. The laser beam may be directed alternatively in each chamber by simply moving a mirror in and out of the laser beam path.

The laser light is provided by an optical parametric oscillator OPO (Continuum Sunlite) pumped by a Nd:YAG laser (Continuum Powerlite 8000) operated at 10 Hz. The signal output of the OPO is used for generation of the UV radiation by frequency doubling in an angle-tuned KDP second-harmonic generation crystal. Thus we get radiation with a pulse energy of 1.5−2 mJ that is tunable within the range 225−350 nm. The pulse length is typically 8 ns.

As beam source we used a pulsed solenoid valve (General Valve Series 9, with a conical outlet) with a nozzle diameter of 500 μm. The valve is driven by a pulse generator (Hewlett-Packard 214B) with pulses of ~75 V amplitude and ~900 μs width. To operate the nozzle between 20 and 180 °C, KALREZ poppets and seals were used. The solid samples were heated in a small oven very near to the nozzle by a flexible heating cable. For temperature control, we used a thermocouple fixed next to the nozzle opening. Helium (Messer Griesheim, purity 99.996%) was used as carrier gas at a typical stagnation pressure of 3 bar.

A digital pulse generator (Stanford Research, DG 535) controls the triggering of the pulses for the laser, the nozzle and the fluorescence detection. This control allows for a variable time delay between the valve opening pulse and the laser firing pulse, which is necessary for exciting the same portion of a supersonic expansion gas pulse at different locations. Thus, one may compensate for the difference in molecular flight time (arrival time) between the different locations at which fluorescence excitation and ionization takes place.

Because only relative intensities are of interest here, the spectra are not corrected for detector sensitivity and no attempt was made to normalize the spectra to the laser power.

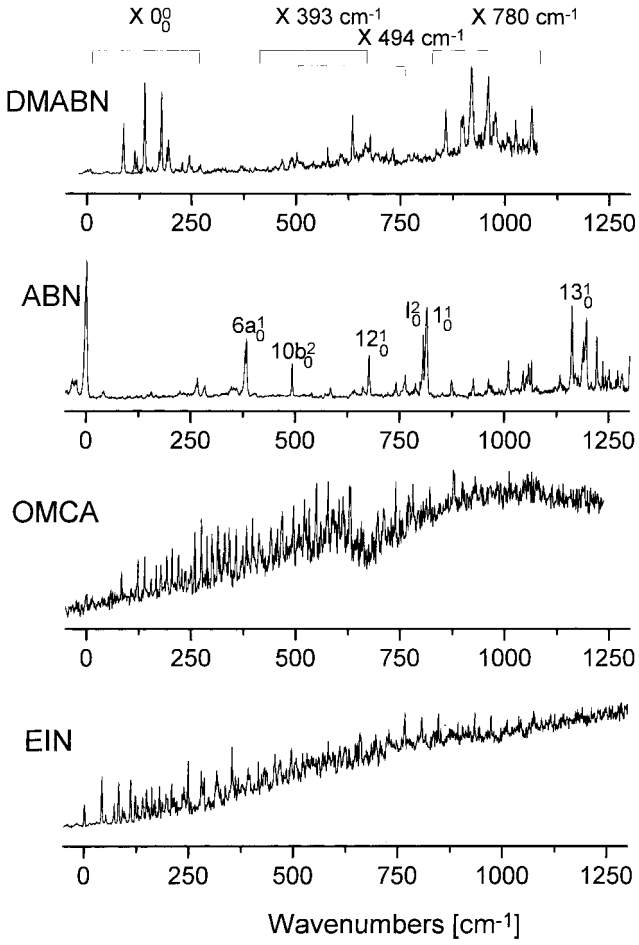

Figure 3. Mass-selected R2PI spectra of DMABN, ABN, OMCA, and EIN. The repeating pattern due to transitions X of the dimethylamino group in combination with fundamentals in the R2PI spectrum of DMABN is indicated. Some prominent transitions in the spectrum of ABN are marked using Varsanyi's notation (amino inversion mode is denoted with I). The decrease of the ion signal at ~650 cm^{-1} in the spectrum of OMCA is due to laser energy fluctuations. The energies of the 0^0_0 transitions are listed in Table 1. The output of the OPO was calibrated by a wavemeter (Atos, LM-007) at regular intervals between the experiments. The spectral bandwith in the visual spectral range was determined to be <0.1 cm^{-1}. The quoted absolute and relative peak positions are accurate to ~0.5 cm^{-1}.

The spectra of DMABEE were recorded using a slightly different setup described in detail in ref 23. Briefly, excitation was provided by the frequency-doubled output of an excimer pumped dye laser (Lambda Physik MG 103SC and LPD 3000, respectively). Fluorescence was detected with a diode array camera (Spectroscopy Instruments, IRQ 700) with 700 pixels.

Among the six compounds studied, ABN, DMABN, and DMABEE were obtained from Fluka (p.a. quality). EIN was synthesized according to a published method[24] in the lab of W. Rettig (Humboldt University Berlin, Germany). OMCA and TMCA were supplied by J. Herbich (Polish Academy of Science, Warsaw, Poland). All compounds were used without further purification.

Results and Discussion

Mass-Selected Resonance-Enhanced Two-Photon Ionization (R2PI) Spectra. The R2PI spectra were recorded for the monomers of all compounds under study and are displayed in Figure 3. The resonant excitation step corresponds to the $S_1 \leftarrow S_0$ transition. Spectra of DMABN, ABN, OMCA, TMCA, and DMABEE are in agreement with previously reported R2PI and fluorescence excitation spectra. To our best knowledge, results on EIN in a supersonic jet were never reported before.

DMABN. The R2PI spectrum of DMABN in the vicinity of the electronic origin is dominated by transitions due to low-frequency modes of the dimethylamino group. The characteristic pattern of these transitions reappears in combination with some fundamental modes at 373, 494, and 780 cm^{-1}. The electronic origin is located at 32257 cm^{-1}. This assignment for the electronic origin is adopted because no evidence for a hot-band transition was detected when recording the spectrum at different stagnation pressures. The R2PI spectrum of DMABN is in agreement with the fluorescence excitation spectra and the R2PI spectra published before.[25,26,27]

The R2PI spectrum of the dimer of DMABN was also recorded (spectrum not shown). In accordance with Bernstein et al.,[28] a slow rise of the ion signal setting in at ~31 250 cm^{-1} with no resolvable features, was observed.

ABN. The most prominent transitions in the R2PI spectrum of ABN are due to the electronic origin and the ring breathing modes 6a, 12, 1, and 13 (in Varsanyi's notation[29]). In contrast to DMABN, an intense 0^0_0 transition is observed for ABN. The fluorescence excitation spectrum of ABN was previously analyzed extensively by Phillips et al.[30,31] Within experimental error, the observed transitions here are in very good agreement with those reported by Phillips et al.[30,31]

OMCA. The R2PI spectrum of OMCA has a rich pattern of shortly spaced transitions throughout the recorded range. Because of the poor signal-to-noise ratio, we were not able to allocate the weak 0^0_0 transition unambiguously. In the fluorescence excitation spectrum reported by Rettschnick et al.[32] the 0^0_0 transition is located at 32 652 cm^{-1}. In this work, the 0^0_0 transition is assigned to the transition at 32 662 cm^{-1}. The spacing between the vibronic bands decreases strongly after the first few vibronic transitions, probably because of combination and sequence transitions. Additionally, vibrations of the methyl group in the ortho-position will contribute to the complexity in the R2PI spectrum.

The absence of a similar peak pattern due to the dimethylamino group like in DMABN, indicates a strong perturbation of the excited-state potential energy surface. Also, the pretwisted conformation in the ground state may contribute to the differences in the R2PI spectra of OMCA and DMABN. In contrast to the spectrum for DMABN, the congestion in the R2PI spectrum for OMCA increases toward higher excitation energies (> 250 cm^{-1}).

TMCA. The R2PI spectrum of TMCA (not shown) shows no resolvable structure, in accordance with the fluorescence excitation spectrum reported by Kajimoto et al.[33] A definite energy for the 0^0_0 transition cannot be given because of the slow rise of the ion signal in the R2PI spectrum.

Kajimoto and co-workers[33] put forward two different explanations for the absence of a sharp 0^0_0 transition: (a) a complex electronic structure in the excited state leading to short lifetimes, and (b) vanishing Franck−Condon (FC) factors due to a large geometrical change upon excitation. The argument of vanishing FC factors seems to be unlikely, when one compares the R2PI spectra of DMABN and TMCA. For DMABN, a 0^0_0 transition is observed, although the dimethylamino group rotates by ~30° in the excited state.[25] For TMCA, the torsional angle of the dimethylamino group relative to the plane of the phenyl ring in the ground state is estimated to be 80°.[34,35] Thus, it is unlikely that a torsional movement (e.g., by 10°) of the dimethylamino group in the excited state leads to vanishing FC-factors.

The congestion in the R2PI spectrum could be due to a shortening of the lifetime (< ps) of the initially prepared state by coupling with another state manifold or due to a high density of states caused by the methyl rotors. However, the absence of a discrete 0_0^0 transition points to a coupling between at least two different electronic states.

DMABEE. The R2PI spectrum of DMABEE (not shown) is in agreement with the fluorescence excitation spectrum observed by Phillips et al.[36] The characteristic low-frequency structure due to the dimethylamino group is observed in the vicinity of the electronic origin. In comparison with the spectrum of DMABN, some additional transitions appear in the region of the electronic origin, which may be related to a decrease in point group symmetry or by coupling of vibronic transitions with the ester group. Altogether, there seems to be only a small perturbation of the dimethylamino group by replacing the nitrile group with an ester group.

EIN. There is nearly no similarity of the R2PI spectrum of EIN with that of 4,4-*N*-(Diethyl)-aminobenzonitrile (DEABN) reported previously.[37] In EIN one valence at the amino nitrogen is an ethyl group, like in DEABN, whereas the other is linked via an ethyl group to the phenyl ring. A similarity could therefore be expected. However, the R2PI spectrum of EIN shows a very complex and congested structure. The transition at 30 753 cm^{-1} is tentatively assigned as the electronic origin. With this assignment, the strength of the 0_0^0 transition would indicate a rather small change in geometry after excitation, which is confirmed by an ab initio calculation.[38] Strong spectral congestion sets in at excitation energies 300 cm^{-1} above the electronic origin. The spectrum is characterized by several low-frequency progressions. A peak assignment is complicated by the size and the low symmetry (C_1) of the molecule. Also, the existence of more than one conformer in the supersonic jet cannot be excluded, because a second conformer would certainly give rise to additional transitions.

The five-membered ring of EIN introduces rigidity with respect to the amino group, but is also capable of giving rise to large-amplitude, low-frequency vibrations similar to those observed in indoline.[39] Like in cyclopentene, the attached five-membered ring resembles a pseudo-four-membered ring due to the C_{phenyl}—C_{phenyl} bond, which acts as single rigid group.[40] The low-frequency transitions may then be attributed to a puckering motion of the methylene group in the 2-position of the five-membered ring and to the amino nitrogen inversion mode. Additionally a "butterfly" bending vibration about the C_{Phenyl}—C_{Phenyl} bond, which is common to both rings, can arise, as observed with indan.[41] Another source for low-frequency transitions is the torsional modes of the ethyl group. A preliminary assignment of the transitions is given in another publication.[38]

Differences in the $S_1 \leftarrow S_0$ R2PI Spectra of the Studied Aminobenzonitriles. The molecules under discussion were and still are of importance in elucidating the origin of dual fluorescence in solution. The different fluorescence behavior of these molecules has been related to the differences in the ground- and excited-state geometries and in the donor—acceptor properties of the groups taking part in the CT.[2a] It is therefore important to determine the changes in geometry and electronic structure of these aminobenzonitriles, that are induced by introducing new substituents.

The R2PI spectra of the six compounds studied give evidence for large differences in their electronic structure from a spectroscopic point of view. The investigated compounds have large differences in the 0_0^0 transition energies and in the extent of congestion in the R2PI spectra. The 0_0^0 transition energy is dependent on the electronic structure of the molecule. Congestion in a spectrum is usually related to the dynamics of the molecule in the excited state [e.g., intramolecular vibrational redistribution (IVR) or radiationless transitions between two electronic states].

TABLE 1. Energy of the 0_0^0 Transitions for the Molecules Studied

molecule	0_0^0 transition (cm^{-1})
EIN	30 753
DEABN[a]	31 817
DMABN	32 257
OMCA	32 662
TMCA[b]	~32 700
DMABEE	33 095
ABN	33 493

[a] From ref 37. [b] No definite energy can be given.

The energies of the 0_0^0 transitions of several aminobenzonitriles are summarized in Table 1. The 0_0^0 transition energy decreases from ABN to DMABN to DEABN. This decrease may be related to the increase of the donor strength with the size of the alkylamino group. The 0_0^0 transition energies of some of the other molecules have been rationalized using a perturbation theory approach introduced by Petruska.[42,43]

A surprising large red shift (~1500 cm^{-1}) of the 0_0^0 transition with respect to DMABN is observed for EIN. Nearly the same shift is observed with respect to OMCA, which, like EIN, has an alkyl-substituent in the ortho-position of the phenyl ring. This result shows that blocking the twisting motion in EIN by linking the dimethylamino group to the phenyl ring via the five-membered ring also leads to a strong perturbation of the π-electron system. Mainly responsible for the perturbation of the π-system and the low energy of the 0_0^0 transition is a large modification in the phenyl ring geometry due to the five-membered ring in EIN.[38] These findings indicate that introducing or changing substituents on DMABN leads to a complex change in the electronic structure (orbital energies), making questionable the attempt to attribute differences in the photophysics solely to differences in the ground-state geometries or to the ability of the twisting motion.

The congestion in the R2PI spectra of EIN and OMCA and the complete loss of structure in the spectrum of TMCA indicate very different potential energy surface(s) for these molecules in comparison with DMABN. In EIN, the number of low-frequency modes leads to a high density of states in the first excited state already in the vicinity of the electronic origin. This high density gives way to a completely different dynamics in the excited state due to the different extent of intramolecular vibrational redistribution (IVR), at least in the gas phase. The congestion in the R2PI spectra of OMCA and TMCA is presumably due to a coupling with a second electronically excited state, which is also indicated by the different emission spectra of EIN and OMCA/TMCA presented next. In the dispersed emission spectrum of EIN, discrete transitions are observed, whereas no resolvable transitions appear for OMCA and TMCA because of a manifold of emitting vibronic states in the second excited state S_2 (vide infra).

One piece of evidence for the TICT hypothesis came from the absence of dual fluorescence in molecules with a blocked twisting motion (e.g., EIN). The differences between EIN and DMABN just outlined above give evidence for the limited comparability between those compounds. This should be taken into account, when the photophysical properties of DMABN

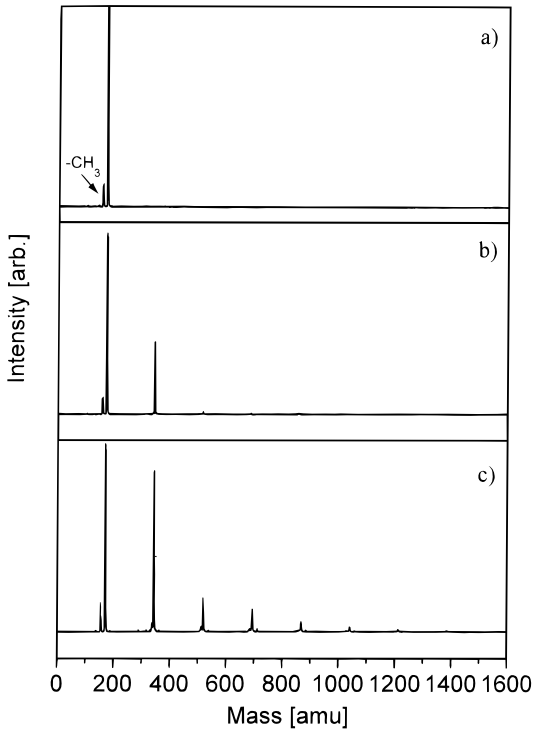

Figure 4. TOF-MS spectra of EIN at three different expansion conditions upon 0_0^0 excitation. The stagnation pressure was 3 bar of He. The nozzle temperature was 80 °C for spectrum a, 100 °C for spectrum b, and 110 °C for spectrum c. The low-intensity peak at the 15 amu reduced mass of the EIN monomer is due the loss of a methly group upon ionization. Typically, each mass spectrum corresponds to 25 single laser shots that are accumulated and averaged in the waveform digitizer.The typical mass resolution is $M/\Delta M \approx 600$ at $M_r = 100$ amu.

and derivatives are compared, as it was done in developing the TICT hypothesis. The problemacy of limited comparability between the DMABN derivatives was already pointed out by Zachariasse et al.[44]

Dispersed Emission Spectra. To control the size distribution of the neutral clusters in the supersonic jet we applied R2PI combined with TOF mass spectrometry. From the mass spectra, information on the excited species in the fluorescence experiment is obtained. The practicability of this correlation was confirmed by the well-known occurrence of excimer fluorescence emission from dimers of fluorene.[45] Synchronously with the occurrence of the fluorene dimer signal in the mass spectrum, we observed excimer emission. Thus it was confirmed that the TOF mass spectrum is representative of the species excited for the fluorescence emission spectrum in chamber 1. A pitfall of this correlation technique is discussed in the section *Spatial Separation of Clusters in a Supersonic Jet*.

In principle, mass spectrometry allows one to obtain information on the size distribution of the neutral clusters in the beam and thus on the species eventually contributing to an emission spectrum. This method presumes that fragmentation induced by the ionization is negligible, which is generally not the case. However, by working under "mild" ionization conditions, one may correlate the species contributing to the fluorescence emission spectra with the cluster ion mass spectra. With resonant two-photon ionization, this makes the use of very low laser intensities and of ionization energies very near to the ionization limit mandatory. By studying the intensity dependence of a mass peak on laser power and excitation wavelength, care was taken to avoid falsification of the mass spectra by fragmentation of larger clusters.

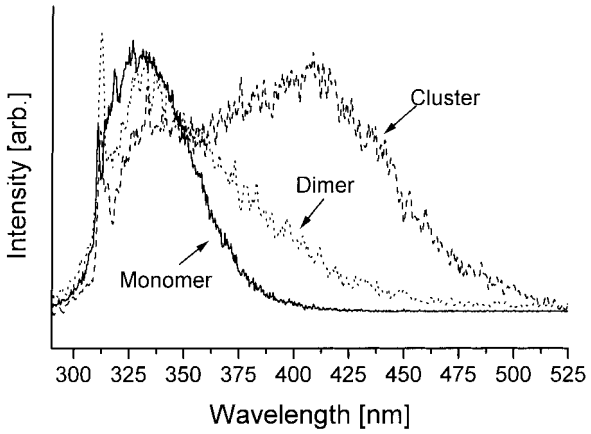

Figure 5. Dispersed emission spectra of jet-cooled DMABN monomer and self-clusters upon 0_0^0 excitation. The nozzle temperatures were 75 and 85 °C for the monomer and dimer/cluster spectra, respectively.

Nevertheless, fragmentation caused by the excess energy in the cluster ion, which is often inherent in the one-color R2PI scheme, cannot be excluded. But even with two-color R2PI, cluster fragmentation may arise even at threshold, when in a vertical ionization transition the clusters are created in a highly excited vibrational state. Then the cluster fragmentation arises due to vibrational relaxation by predissociation.[46] Because of the high binding energies in clusters of polar molecules and in the absence of hydrogen bonding via the π-electron system, the cluster fragmentation probability should be reduced. The fragmentation efficiency of a cluster is governed by the change of geometry between the S_1 and the ion state, which is assumed to be small for the polar aminobenzonitriles. Due to the propensity rule ($\Delta\nu = 0$) for the change of the vibrational quantum number ν, it is expected that the ion is created with low vibrational excitation in the R2PI process when the vibrationless S_1 state is excited.[47] This is even the case for large excess energies, which is expected to be the case here. This excess energy is then carried away by the photoelectron. Therefore, fragmentation is not expected to become a fully quantitative process for the homogeneous clusters of the molecules studied in this work.

Figure 4 shows three typical TOF mass spectra of EIN representing different cluster size distributions in the supersonic expansion. The size distribution was basically varied by changing the sample/nozzle temperature and by adjusting the time delay between the laser pulse and the opening pulse of the valve. The gas pulse was sampled in the middle of its temporal profile.

The mass spectra in Figure 4 show the cluster size distribution under three markedly different expansion conditions. Low sample temperature and short nozzle pulses were employed for a size distribution containing only monomers (Figure 4a). Increasing the sample temperature and hence vapor pressure and the length of the gas pulse leads to a cluster size distribution consisting of mainly monomers and dimers (Figure 4b). A further increase of these parameters leads to the formation of clusters with sizes up to $n < 10$ (Figure 4c).

Figures 5−12 report the dispersed fluorescence emission spectra for all aminobenzonitriles studied. For all molecules, the emission spectra were recorded for each of the three typical cluster size distributions, as shown representatively for EIN in Figure 4. The prevailing cluster size distributions in the mass spectra are denoted in the following emission spectra by the abbreviations monomer (Figure 4a), dimer (Figure 4b) and cluster (Figure 4c), respectively. The excitation wavelength was

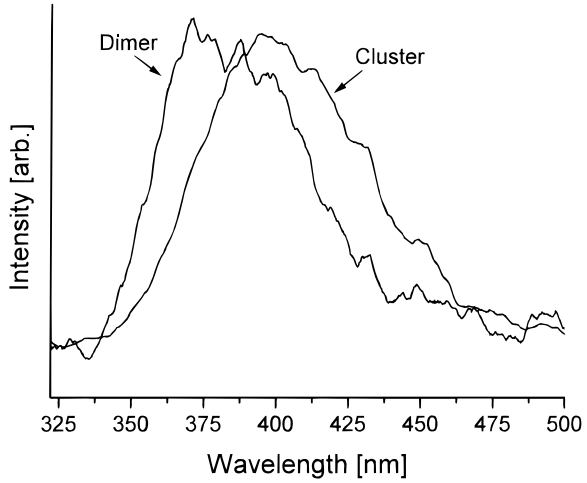

Figure 6. Dispersed emission spectra of jet-cooled DMABN self-clusters upon excitation red-shifted by 600 cm^{-1} to the 0_0^0 transition. The nozzle temperature was 95 °C. Due to the low intensity, the spectra were slightly smoothed by digital filtering.

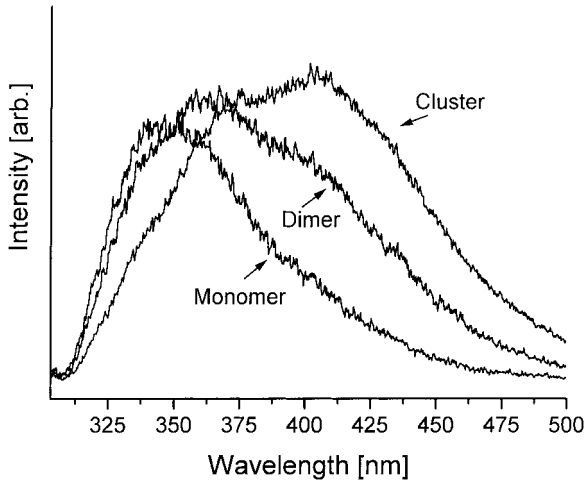

Figure 7. Dispersed emission spectra of jet-cooled OMCA monomer and self-clusters upon excitation at 300 nm in the vicinity of the electronic origin. The nozzle temperatures were 90 and 100 °C for monomer and dimer/cluster spectra, respectively.

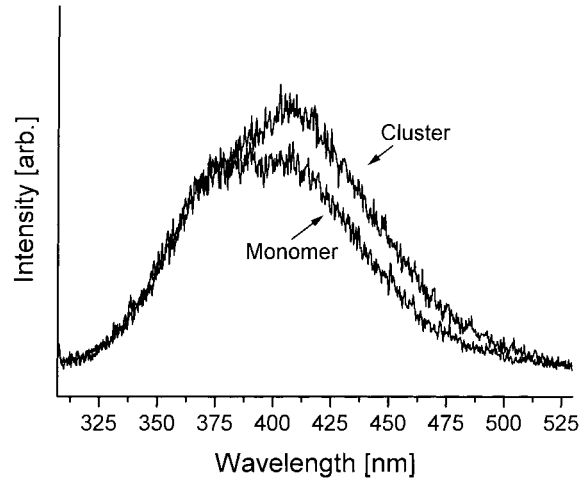

Figure 8. Dispersed emission spectra of jet-cooled TMCA monomer and self-clusters upon excitation at 301 nm. The nozzle temperatures were 100 and 115 °C for monomer and cluster spectra, respectively.

the 0_0^0 transition of the respective monomer, except as indicated otherwise. The emission maxima and bandwidths of the fluorescence bands of all compounds studied are given in Table 2. The spectra are approximately normalized to equal intensity for the respective maximum.

DMABN. The fluorescence emission spectra of a homogeneous supersonic expansion of DMABN in helium strongly depend on the size of the excited clusters. For the monomer a single broad, not fully resolved, emission spectrum with a maximum at 330 nm is observed. When aggregates start to grow up in the expansion, a second red-shifted emission band develops (Figure 5). With a cluster size distribution containing only monomers and dimers the new red-shifted emission has a maximum at 390 nm. Formation of additional $(DMABN)_n$ clusters with $n \geq 3$ shifts this maximum to 410 nm. The two different red-shifted emission maxima become clearly visible, when the monomer emission spectrum is subtracted from the dimer and the clusters spectrum, respectively (not shown).

If one compares the emission due to the monomer component with that of the clusters, the very different particle densities in the jet represent a problem. To distinguish the weak cluster fluorescence from the very strong monomer emission, the excitation wavelength was shifted by 600 cm^{-1} to the red side of the electronic origin of the monomer (Figure 6). By this shift, only clusters and hot monomers are excited. Thus, the emission originating from the monomer is largely supressed. In the case of the red-shifted excitation, nearly no LE fluorescence is observed for the dimers and larger clusters. The emission arising from the dimer is red shifted, with the center of emission at 390 nm (which corrsponds not to the maximum intensity at shorter wavelengths). With increasing cluster size, the emission maximum shifts a little further to the red to 410 nm. Obviously, the emission maxima are independent of the excitation wavelengths employed.

The emission maximum at 390 nm was tentatively assigned to the DMABN dimer by Phillips et al.[48] These authors used the nozzle temperature for an estimate of the cluster size distribution. The red-shifted emission due to self-complexes of DMABN has been also observed by Peng et al.,[37] without a mass analysis of the jet.The present experiments give evidence that this band is indeed due to dimers.

OMCA. The dispersed emission spectrum of the monomer of OMCA (Figure 7) has no resolvable vibrational structure (at least at the given resolution of the monochromator employing the 300 g/mm grating). Under expansion conditions with dimer formation, a red-shifted emission with a maximum at 405 nm is observed. The formation of larger clusters shifts the spectrum slightly further to the red and leads to an increase of intensity for the red-shifted emission band.

The absence of discrete features in the emission spectrum of the OMCA monomer is in striking contrast to EIN (vide infra). The density of FC-allowed states in the ground state of OMCA certainly does not exceed that of EIN, leading to the conclusion that the emission originates from a larger manifold of vibronic states. Because a transition in the region of the electronic origin was excited, this means, that a coupling with another electronically excited state has occurred. However, in case of intense activity of the low-frequency modes (e.g., methyl pseudorotation), the monochromator resolution may be not sufficient to reveal discrete features. A low-resolution emission spectrum of the monomer of OMCA was also reported by Rettschnick et al.[32]

TMCA. The fluorescence spectrum of TMCA, depicted in Figure 8, is somewhat special. The very broad emission spectrum of the monomer has a maximum at 390 nm, which shows in addition a slight but reproducible dip at 395 nm. The occurrence of aggregates in the expansion alters the intensity

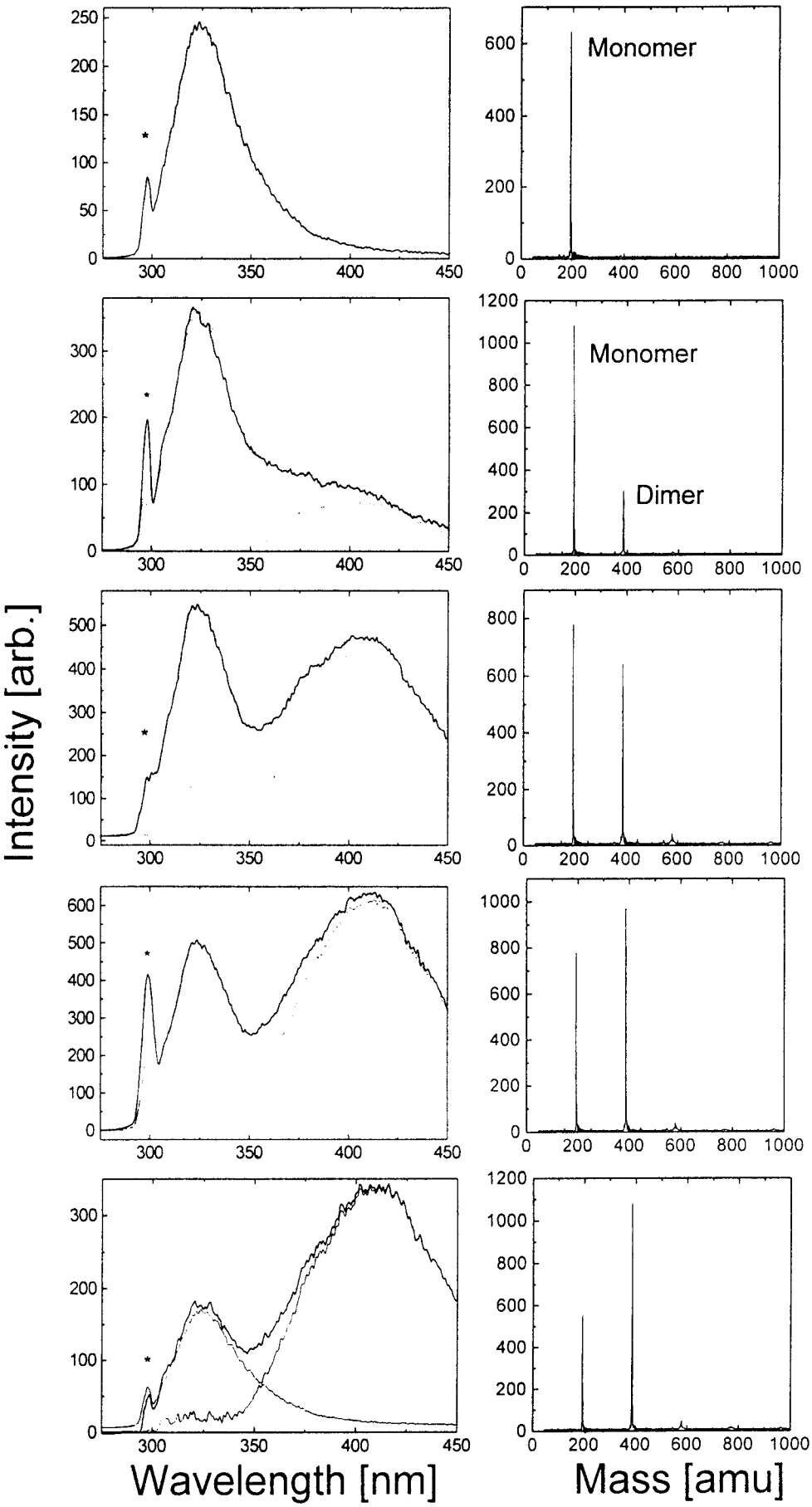

Figure 9. Dispersed emission spectra of jet-cooled DMABEE monomer and self-clusters upon nonresonant excitation at 298 nm. The nozzle temperature was 110 °C for monomer and dimer/cluster spectra. The cluster size distribution was varied by changing the operating conditions for the nozzle (amplitude and length of drive pulse).

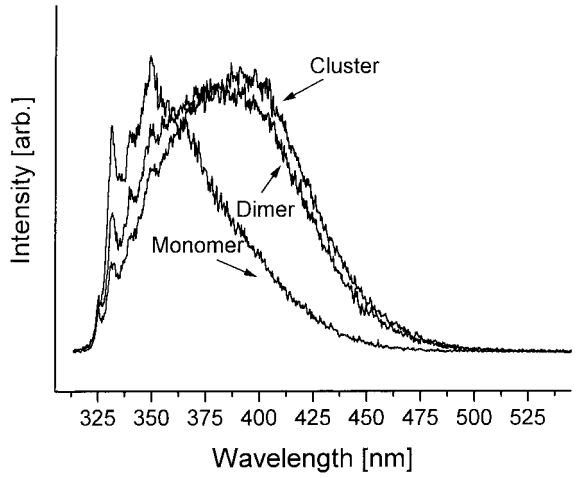

Figure 10. Dispersed emission spectra of jet-cooled EIN monomer and self-clusters upon 0_0^0 excitation. The nozzle temperatures were 80 and 110 °C for monomer and dimer/cluster spectra, respectively.

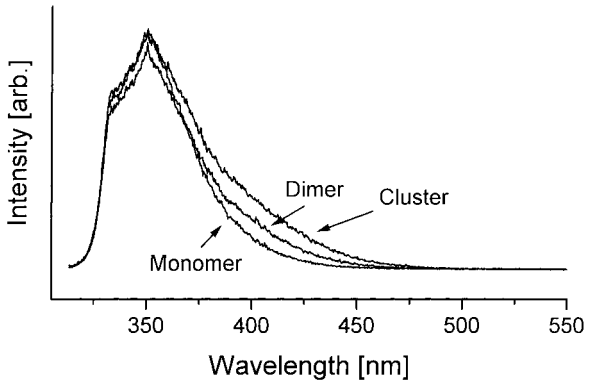

Figure 11. Dispersed emission spectra of jet-cooled EIN monomer and self-clusters upon exciting with large excess excitation energy 1500 cm^{-1} above the electronic origin at the same expansion conditions as for Figure 10.

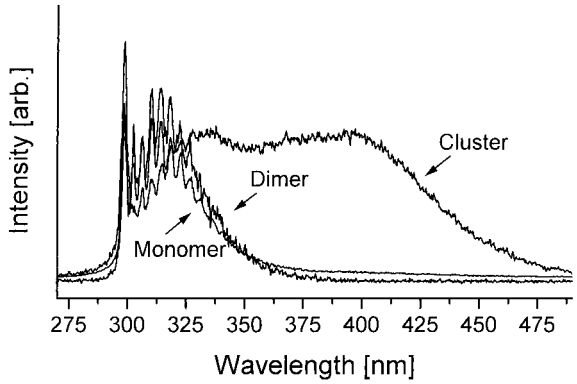

Figure 12. Dispersed emission spectra of jet-cooled ABN monomer and self-clusters upon 0_0^0 excitation. The nozzle temperatures were 85 and 95 °C for monomer and dimer/cluster spectra, respectively.

of the red part of the monomer emission spectrum only slightly. However, the broad monomer emission may mask an additional weak emission band due to larger aggregates of TMCA.

It is known from the literature that the monomer emission spectrum depends on the excitation wavelength and consists of a superposition of the emission from the S_1 and S_2 state.[27] Kajimoto et al.[27] attributed the fluorescence band of the monomer excited at $\lambda_{exc} > 305$ nm to the CT state (S_1 in this case). The CT nature of the S_1 emission was deduced from experiments in solution with different solvents. Excitation of the monomer at shorter wavelengths shifts the emission maximum to the blue ($\lambda_{max} = 335$ nm at $\lambda_{exc} = 278$ nm). This change was attributed to emission originating from the S_2 state.[27] A similar dependence on the excitation wavelength was also observed by us (spectra not shown).

TABLE 2. Emission Maxima of the LE and the Red-Shifted Emission Spectra and the Shift between the Maxima

substance	maximum of local emission (nm)	maximum of red-shifted emission (nm)	fwhm of local emission (cm^{-1})	shift LE/CT emission (cm^{-1})
DMABN	330	390/410	4400	4660/5900
ABN	319	395	3900	6030
OMCA	346	405	5870	4210
TMCA	–	400	–	–
EIN	350	390	4080	2930
DMABEE	325	410	3280	6380

DMABEE. The spectrum of the DMABEE monomer has a single fluorescence emission band with a maximum at 325 nm. A second red-shifted emission band with a maximum at 410 nm develops synchronously with the occurrence of the dimer signal in the mass spectrum. The correlation between the mass and emission spectra is displayed in Figure 9. The red-shifted emission band was already observed by Phillips et al.[36,49] and attributed to dimers. But these authors could not exclude chromophore−water complexes in their supersonic expansion.

It was postulated, that in DMABEE the lowest excited state is of different symmetry than in DMABN due to the better acceptor properties of the ester group.[21] In the ester, the initially excited state should have the same symmetry as the TICT state (both L_a), whereas in DMABN, the LE state and the TICT state are of different symmetry (L_b and L_a, respectively). If this symmetry is the case, an adiabatic transition from the LE state into the CT state would be expected for the ester. However, under jet-cooled conditions, no red-shifted emission is observed for the monomer. A possible explanation for the absence of the anomalous fluorescence of the monomer could be a barrier between the LE and the CT states. On the other hand, it is possible, that in the gas phase the lowest excited state of DMABEE is of L_b symmetry, like for ABN and DMABN. Studies on 4-(dimethylamino)-benzoic acid methyl ester (DMABME) by Wallace et al.[50] and by Jouvet et al.[51] support this argument. For this molecule, which is very similar to DMABEE, no evidence for pure L_a symmetry of the FC-excited state has been found.

EIN. The monomer spectrum of EIN shows an unresolved fluorescence spectrum with a maximum at ∼350 nm (Figure 10). Superimposed on the emission band are three partially resolved transitions on its blue side. The spectrum is assigned to the emission from the LE state. The emission spectrum at higher resolution is reported in a separate publication.[38] With the occurrence of dimers in the supersonic expansion a second red-shifted emission band develops with a maximum of ∼400 nm. Formation of larger clusters shifts the emission spectrum only slightly.

With increasing excitation energy a quenching of the red-shifted emission fluorescence is observed (Figure 11). At excitation energies 1500 cm^{-1} above the electronic origin of the monomer, the emission spectrum of the monomer has lost all spectral features, presumably due to IVR in the excited state and a large density of states in the ground state. The red-shifted fluorescence intensity due to the clusters is no longer prominent. The emission spectra with excess energy excitation have been recorded with a rather large stepwidth between the respective

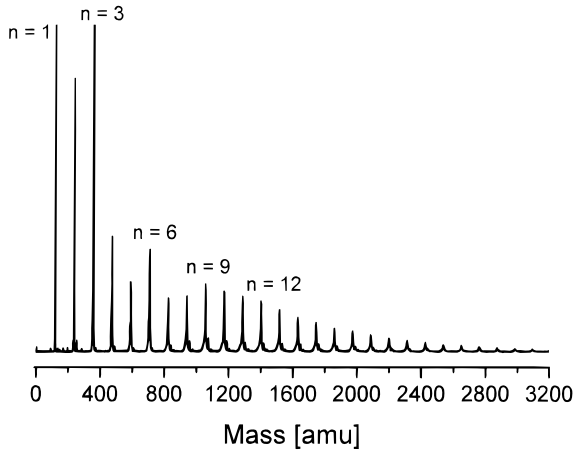

Figure 13. TOF mass spectra of ABN clusters upon excitation at the electronic origin of the monomer. The displayed intensity of the monomer peak is reduced.

excitation wavelengths. Therefore, it is not known whether the quenching process has a sharp onset or takes place in a gradual way with increasing excitation energy. However, a slight quenching of the red-shifted emission seems to take place already at 300 cm^{-1} above the electronic origin of the monomer.

ABN. The emission spectra of ABN at different expansion conditions are depicted in Figure 12. The monomer emission spectrum at low resolution has a maximum at 320 nm. The spectrum of the ABN monomer was also reported by Phillips et al.[30,31]

The dependence of the emission spectra on the cluster size distribution doesn't follow the general pattern observed and already discussed for the other molecules. At expansion conditions where only small aggregates ($n \leq 3$) are observed in the mass spectrum, an additional red-shifted component is not observed in the emission spectrum. Also, at excitation energies 1600 cm^{-1} above the electronic origin of the monomer, a red-shifted emission due to the small clusters cannot be induced. Only with the appearance of larger aggregates ($n \geq 4$) does a strong red-shifted emission show up, with a maximum at 395 nm. The observed red shift for this component relative to the LE emission is the strongest for all aminobenzonitriles studied in this work.

It is worth noting that the TOF mass spectra of the ABN jet expansion show a remarkable irregularity in the cluster size distribution. The intensities of the $(ABN)^+_n$ clusters, with $n =$ 3, 6, 9, and 12, have higher or at least equal intensity than the neighboring cluster of lower mass (Figure 13). Such *n*-values are called magic numbers. In the experiment they are independent of the excitation wavelength and, hence cannot be due to a resonance effect in the ion yield.

Discussion on the Origin of the Red-Shifted Emission Bands. By correlating the mass and emission spectra we could give evidence that the observed red-shifted emission is due to the formation of self-complexes. With the exception of TMCA and ABN, this red-shifted component appears synchronously with the dimer species in the expansion. This result is documented clearly by the corresponding mass spectra. By using our experimental setup, we can definitely rule out heterogeneous species, such as $(DMABN)_n$−water clusters, as a contamination responsible for the red-shifted fluorescence in the homogeneous expansion. However, chromophore−water complexes were occasionally observed in the expansion. In those cases, the substance in the nozzle was exchanged or the experiment delayed until the water disappeared in the mass spectrum.

The origin of the red-shifted emission cannot be explained a priori. A conclusion may be drawn only by comparing the emission spectra of the related molecules studied in this work. Following the argument given by Phillips et al.[2c,49] the red-shifted fluorescence of the DMABN dimers can be caused either by a transition into an excimer state or into a TICT state of one chromophore enabled in the dimer by its polar partner. Alternatively to the twist of the dimethylamino group in the excited state, a different conformational relaxation may occur (e.g., bending of the nitrile group, RICT hypothesis).

All these models have in common that the red-shifted emission is rationalized by transitions terminating on a repulsive ground-state PES at the geometry of the relaxed excited state. The similarity of the models at this point make a conclusive discrimination of the various possibilities for dual fluorescence difficult. The models differ, however, in the proposed change of geometry in the excited state, which is difficult to examine both experimentally and theoretically.

The red-shifted fluorescence is observed for homogeneous clusters of all compounds studied (except TMCA). As outlined in the discussion of the R2PI spectra, all molecules differ strongly in geometry and electronic structure. For the differences in geometry see also ref 38. The observation of a red-shifted emission for all six different compounds rules out the explanations given for dual fluorescence in solution.

The occurrence of the red-shifted emission for aggregates of ABN and EIN in addition to DMABN indicates that a TICT state formation cannot account for the anomalous fluorescence of the clusters. Neither ABN nor EIN give rise to dual fluorescence in polar solutions. The absence of dual fluorescence for ABN is explained within the TICT model by the reduced donor properties of the amino group (due to the missing methyl groups) and in the case of EIN by the blocked twist of the donor group. The solvent-induced pseudo-Jahn−Teller coupling model proposed by Zachariasse rationalizes the absence of dual fluorescence of ABN by a large energy separation of the S_1 and S_2 states and by the limited conformational flexibility of the amino group in EIN.[10] It should be pointed out that the bending of the nitrile group in the excited state is possible for all molecules studied, except for the ester DMABEE. The RICT model should therefore also not account for the anomalous fluorescence in the jet.

Hence, all three models seem not to be able to account for the observations made in this supersonic jet study. The most plausible rationale remaining is an excimer mechanism as the origin for the anomalous fluorescence. Support for the excimer origin of the dual fluorescence arises from the absence of a red-shifted (excimer) emission for small clusters ($n \leq 3$) of ABN and the peak intensity distribution in the corresponding mass spectra showing magic numbers (Figure 13). We propose for the dimer and trimer of ABN a structure that is not favorable for the efficient formation of an excimer geometry. It is plausible to assume for the dimer a geometry with a (nearly) planar head-to-tail conformation stabilized by a hydrogen bond between the amino hydrogen and the nitrogen of the nitrile group. For the same reasons, a cyclic structure for the trimer is proposed. Although the structural proposals are not yet proven, the preference of certain cluster sizes with a periodicity of three molecules cannot be rationalized by the alternative sandwich-like structure. A planar structure for the similar benzonitrile dimer due to hydrogen bonds was proposed earlier by Kajimoto et al.[52] This kind of hydrogen bonding has also been detected by X-ray analysis in the crystal structure of ABN by Heine et al.[53] and in the acetonitrile dimer by Rühl.[54] The

formation of intermolecular hydrogen bonds leading to the proposed structures for the ABN dimer and trimer is only possible for ABN but not for the other molecules studied in this work. Thus, the nonsandwich conformation would account for the absence of anomalous fluorescence for small clusters of ABN in these experiments. A sandwich structure is expected to be more likely for larger clusters of ABN ($n \geq 4$) for which the red-shifted emission is indeed observed. If excimer formation and sandwich structure are synonymous, the red-shifted excimer emission band is thus expected to appear only in larger clusters. From the absence of dual fluorescence for the ABN dimer and trimer it is concluded that a cluster with sandwich conformation of at least two molecules is a *conditio sine qua non* for the observation of dual fluorescence. This conclusion is a direct hint for an underlying excimer mechanism for the red-shifted emission.

Evidence for excimer emission is also provided by the fluorescence of the DMABEE dimer. The red-shifted emission band for the dimer was also observed in solution by Phillips et al.[36] The emission was attributed to excimer emission due to its concentration dependence. The emission maximum in a nonpolar solution has been observed at 410 nm, which is nearly identical to the emission wavelength observed here in the jet. However, Brown et al.[55] attributed this red-shifted emission in solution also to the formation of dimers but without postulating an excimer state.

For the clusters of TMCA, no convincing evidence for excimer emission has been found. This result may be related to the sterical hindrance due to the two additional methyl groups, which may prevent the efficient formation of an excimer geometry. Also the special electronic structure of TMCA may account for the absence of excimer emission. On the other hand, eventually the excimer emission is only weak and masked by the broad emission of the monomer.

For some of the systems studied an additional or alternative mechanism to excimer formation for the observed red-shifted band cannot be ruled out completely (e.g. TICT or RICT). However, it is not very likely that for DMABN, for example, a different mechanism should cause a similar dual fluorescence as for EIN. Thus, it is more likely that excimer formation takes place for all molecules studied because it is difficult to rationalize why excimer formation should not take place.

The limited comparability of the molecules studied due to their different electronic structure and geometry is of minor relevance in the assumed excimer mechanism. In fact, the limited comparability supports the assumption of the excimer mechanism. The energy of an excimer state is, apart from the intermolecular distance, determined by the transition moment and the donor/acceptor properties of the molecule. Both properties are very similar for the group of molecules studied. The acceptor system is the benzonitrile moiety for all molecules studied (except DMABEE). Furthermore, all molecules exhibit a comparable increase of the dipole moment (charge redistribution) in the LE state, and the lowest excited state is of the L_b type with a weak transition dipole moment (except TMCA). If, however, any intramolecular process would be responsible for the red-shifted emission, a dissimilar emission behavior due to the differences in monomer geometry is expected, which is not observed.

For the quenching of the excimer emission of the dimer (and clusters) of EIN at large excess excitation energies two explanations are offered. The quenching could be due to fragmentation, which would have to occur in the $S_{1(?)}$ state on a slower time scale than the R2PI process, because the dimer is still observed in the mass spectrum. Another possibility is the relaxation of the system into a dark state. This dark state could correspond to another exciton state at higher energy, out of which emission to the ground state is prohibited (vide infra).[56]

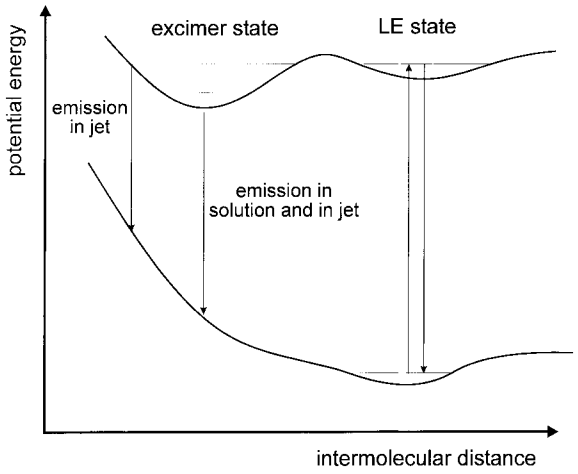

Figure 14. Potential energy surface(s) for excimer formation.

A red-shifted emission due to small aggregates of DMABN and related compounds has also been found in concentrated solution by Rotkiewicz et al.[57] In low-temperature experiments in nonpolar solvents, these authors observed a red-shifted emission band for DMABN, OMCA, and 1-methyl-2,3-dihydroindole-5-carbonitrile (MIN; comparable to EIN). The anomalous fluorescence has been attributed to the formation of dimers. The formation of excimers was neither proven nor excluded. The emission maxima in solution observed by Rotkiewicz et al.[57] are similar to those observed here in the jet. Thus, the clusters in the jet obviously mimic the process observed in *concentrated* solution.

An aromatic excimer consists of two monomer units M in a strongly bonding excited electronic state with a nonbonding ground electronic state (in solution).[58] The excimer state is stabilized by configuration interaction with charge resonance states ($M^-M^+ \Leftrightarrow M^+M^-$) and exciton resonance states ($M^*M \Leftrightarrow MM^*$). The excimer fluorescence is red-shifted and structureless due to the emission from an attractive excited excimer state to a repulsive ground-state PES.

Figure 14 displays schematically the PES of a vdW dimer in the gas phase. In a supersonic jet, a shallow minimum in the ground-state potential curve leads to the formation of weakly bound vdW dimers due to the low internal temperatures in the jet. The upper potential curve has a minimum near the geometry of the ground-state vdW dimer and a deeper minimum for the excimer state at a smaller intermolecular separation of the monomer units. The shape of the upper PES is the result of the coupling between the lower exciton resonance diabatic state and the lower charge resonance diabatic state. The relative contributions of exciton resonance and charge resonance to the excimer stabilization is still a controversy.[59,60] The stabilization of an excimer[58] due to charge resonance is given by the potential energy function

$$V = \mathrm{IP} - \mathrm{EA} - \mathrm{C(r)} \qquad (1)$$

where IP is the ionization potential, EA is the electron affinity of one monomer subunit, and C(r) is the coulomb attraction. The stabilization due to exciton resonance in the dipole−dipole approximation is given by the potential energy function

$$V = E \pm \mathbf{M}^2/r^3 \qquad (2)$$

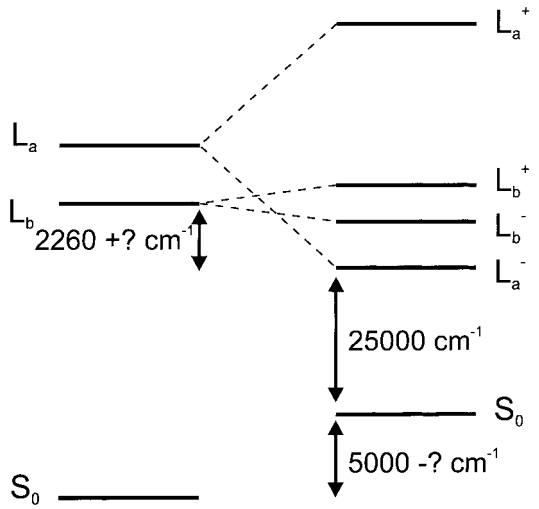

Figure 15. Schematic diagram of the estimated DMABN excimer stabilization due to exciton resonance interaction. The exciton splitting of the L_b state is only 39 cm^{-1} due to the low oscillator strength. The in-phase and out-of-phase combinations of the exciton resonance states are signed by L^+ and L^-, respectively. An ideal sandwich geometry is assumed for the excimer. The (unknown) energy contribution of charge resonance interaction is indicated by the question mark.

where **M** is the transition dipole moment, E is the unperturbed excited-state energy for one monomer subunit, and r is the intermolecular distance between the monomer units in the excimer. The condition on the excimer geometry for a nonvanishing exciton interaction is a parallel orientation of the two subunits, which leads to parallel-oriented transition moments. In case of perpendicular transition moments, the exciton interaction vanishes. The relative orientation in a parallel geometry determines the sign in eq 2. In case of an ideal sandwich conformation, the out-of-phase combination (−) of the (M^*M) and (MM^*) wave functions is the lower exciton state, whereas for an in-plane head-to-tail orientation, the in-phase combination (+) is the lower exciton state. For parallel transition moments, emission from the out-of-phase exciton state to the ground state is forbidden and for the in-phase exciton state emission is allowed.[56] However, the (forbidden) emission from the out-of-phase exciton state is expected to have a similar quantum efficiency as emission from the L_b state, which is also only weakly allowed.

In an estimation of the stabilization due to exciton resonance interaction for the DMABN dimer, both the L_b and the L_a states have to be considered. The much larger transition dipole moment to the L_a state makes the exciton splitting of this state the dominant stabilization. Employing the computed values for the oscillator strengths and excited-state energies from ref 2b, an exciton resonance stabilization energy of 0.28 eV of the excimer state relative to the L_b state is obtained.[61] With an excimer emission energy of 3.18 eV (∼390 nm), this energy leaves 0.6 eV for the repulsion energy in the ground state plus an additional but unknown stabilization in the excited state due to charge resonance interaction (Figure 15). An energy of 0.6 eV is too high to be exclusively due to the repulsion in the ground state, making a significant contribution of charge resonance in the stabilization of the excimer likely. This likelihood is supported by the net stabilization of an intermolecular CT already at an intermolecular distance of ∼4 Å, which is calculated with eq 1 and by assuming an IP* of 3.51 eV (= IP − L_b) for the excited DMABN and approximating the EA of DMABN by the value of 0.26 eV for benzonitrile.[62]

The energy of the excimer emission for the DMABEE dimer, which is 0.21 eV (∼1700 cm^{-1}) smaller than for $(DMABN)_2$, can also be rationalized within this excimer model. The L_b and L_a states are separated by 0.19 eV (∼1500 cm^{-1}) in DMABN, but are in close proximity in DMABEE.[21] This situation leads to the stronger stabilization of the DMABEE excimer due to the exciton splitting of the L_a state (assuming similar oscillator strengths for the transitions to the L_b and L_a states).

The actual dynamics of the initially excited vdW dimer depends on the energy gap and the coupling strength between the LE and the excimer state. For the coupling strength, a strong dependence on the intermolecular geometry is expected.[63,64] The LE geometry of the vdW dimer of DMABN is expected to resemble a sandwich-conformation with opposite orientation of the two chromophores. Such a conformation is expected in view of the large dipole moment of the chromophore and would greatly facilitate the formation into the excimer geometry. Due to the absence of resolvable features in the R2PI spectrum of the DMABN dimer, no hints on the exact geometry of the dimer or on the simultaneous existence of several isomers are obtained. The missing vibronic structure may indicate a fast relaxation from the LE state into the excimer state caused by a strong coupling between these states, which leads to a (nearly) barrierless transition into the excimer state on the excited-state PES.

For the ABN dimer the barrier between the LE state and the excimer state is obviously so large that even at large excess excitation energies (>1600 cm^{-1}) a transformation into the excimer state cannot occur. This result is in accordance with the proposed structure for the ABN dimer, which implies a low coupling strength.

From the proposed excimer model, the following picture of the photophysics in a supersonic jet of the aminobenzonitriles studied is obtained (Figure 14).

The excimer formation involves the photoexcitation of the ground state vdW dimer into a locally excited state. Relaxation to the excimer state occurs via a molecular rearrangement by passing over the energy barrier or in a barrierless process. This relaxation may be affected by excess internal energy or by tunneling through the barrier. Due to the nature of exciton and charge resonance interaction, the intermolecular distance and orientation of the monomer units in the excimer state differ strongly from the locally excited state. Therefore, the ground-state potential curve is repulsive at the excimer geometry, causing a broad and red-shifted emission.

By the transition from the LE state to the excimer state, the cluster is produced with an intermolecular coordinate that is highly vibrationally excited. Emission originating from such a state is substantially red-shifted due to FC arguments.

The FC factors are expected to be largest at the classical turning points of the highly vibrational excited state. Then the transitions are more intense at the turning point at short intermolecular distances terminating on a strongly repulsive part of the ground-state PES.

Clearly, this one-dimensional picture is too simplistic. Additionally, IVR to the other inter- and intramolecular low-frequency modes is likely to occur in the excited state. Emission from a cluster, where extensive IVR has occurred, can also be described by the same model. In this case the intermolecular coordinate in Figure 14 has to be interchanged by another inter- or intramolecular low-frequency mode. However, it is not unreasonable to assume, that an intermolecular stretching coordinate is of greatest importance for the red-shifted emission due to the different nature of the intramolecular low-frequency

modes in ABN, DMABN, and EIN. The number and the kind (coupling strength) of these low-frequency modes in those three molecules is largely different and IVR to these coordinates accounts therefore presumably not predominantly for the red shift. But they account probably for the different shifts of the emission maxima between LE and excimer emission of those molecules.

The here observed similarity between the fluorescence spectra of the dimers and of larger clusters indicates that the clusters in the excimer state consist of a strongly bound dimeric core, where the excitation is localized. The additional ground state molecules of the cluster are weakly bound to this core excimer and cause only minor changes in energy and FC factors. Such a core structure of excimer clusters was found previously for the tetramers of naphthalene.[65]

The proposed excimer model also accounts for the similar energies of the red-shifted emission due to dimers and clusters in the jet and in solution, as observed by Rotkiewicz et al.[57] In solution, collisional relaxation takes place, resulting in emission from the minimum of the excimer PES. For clusters in a supersonic jet, IVR in the excited state may take place and emission can therefore arise at the same intermolecular distance than in the solution phase. However, because vibrational relaxation is arrested under isolated conditions, excimer emission in a jet is usually broader than in solution. On the other hand, if excimer emission originates from a smaller intermolecular separation, the increase in ground state repulsion energy compensates for the impossibility of energy relaxation in the excited state. In zero-order approximation, the repulsive part of the PES for ground and excited states respectively, are equal in slope. The energy differences between the excimer state and the ground state at the respective intermolecular distances for emission in the jet and in solution are therefore expected to be similar. Thus, similar emission spectra are observed in the jet and in solution.

Implications for the Dual Fluorescence in Solution. The excimer mechanism found for the jet-cooled self-complexes points strongly to the same mechanism being responsible for dual fluorescence in *concentrated* solutions of DMABN. The anomalous fluorescence in solution with high concentrations of the chromophore can therefore be assigned to the formation of excimers. The formation of a TICT state in the dimer can be excluded. In dilute solutions, however, different mechanisms (e.g., TICT or exciplex formation) should be responsible for the phenomenon of dual fluorescence.

Spatial Separation of Clusters in a Supersonic Jet. Already at the early stages of research with molecular beams it was found that the heavier components of a gas mixture are enriched on the beam axis, whereas the lighter components are also found in the periphery.[66,67] From different experiments reported in the literature, several mechanisms were proposed. Becker et al.[68] and Waterman et al.[69] explained the separation by a larger thermal velocity of the lighter component. The corresponding velocity is inversely proportional to the respective cluster mass.[70] Therefore, lighter species have a larger perpendicular component of motion, causing a stronger lateral spreading. This phenomenon was termed Mach number focusing.

Later, Becker et al.[71] rejected his explanation in favor of a model based on pressure diffusion. Recently Gedanken et al.[72,73] observed the separation effect for clusters of organic molecules in a supersonic jet using mass spectrometry. They found that similar principles apply for clusters as for a mixture of gases with different molecular weight.

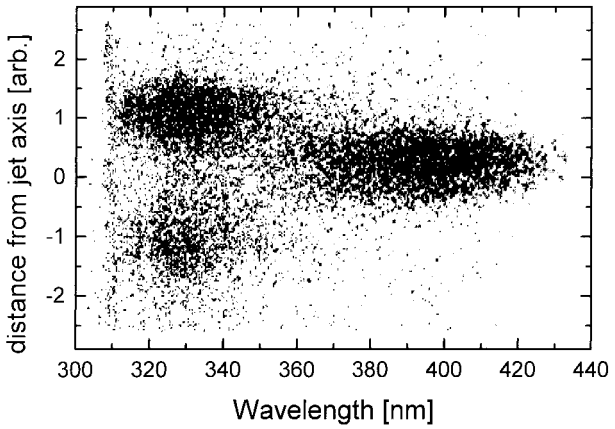

Figure 16. CCD image of the dispersed fluorescence emission of a homogeneous jet expansion of DMABN. Larger clusters emitting at 410 nm are on the jet axis; monomer emission at 330 nm takes place from the outer sphere of the jet. The full lateral dimension of the *y*-axis (vertical to the jet-axis) of the CCD-detector is estimated to correspond to ~5 mm width of the object image.

In addition to the separation of components vertically to the jet direction there is a separation parallel to the jet axis (velocity slip). The velocity slip is due to different terminal velocities for molecules with large differences in collision cross section and mass. This type of separation is of minor importance and is not considered here.

The use of a CCD camera with a large image array for detecting the fluorescence allows one to observe the spatial separation of clusters of different sizes in a supersonic jet. In this study, the Mach number focusing shows up by the different fluorescence behavior of bare and self-complexed DMABN. The two-dimensional CCD detector used for fluorescence detection at the ouput of the spectrograph allows one to observe both the wavelength dispersion and the lateral distribution of the emitting species perpendicular to the jet direction.[74] Figure 16 shows such an image received after exciting and dispersing the fluorescence of a jet expansion of DMABN containing monomers and clusters. The long axis of the image corresponds to the wavelength axis, whereas the short axis corresponds to the lateral density distribution perpendicular to the jet axis. Dark shaded areas in the image correspond to high fluorescence intensities. The CCD image is not uniform because the different emission maxima of the monomers and the clusters and their spatial dispersion.

As shown in Figure 5, the monomer emission of DMABN peaks at $\lambda = 330$ nm, whereas clusters have an emission maximum at $\lambda = 410$ nm. The CCD image shows the accumulation of the clusters, that emit the red-shifted fluorescence on the jet axis (emission in the middle of the CCD image). Emission at shorter wavelengths, assigned to the LE emission of the monomer, has a much stronger angular distribution and arises mainly from the outer parts of the supersonic jet (emission at top and bottom of the CCD image). In this qualitative evaluation, approximately equal quantum efficiencies are assumed for monomer and cluster emission.

This Mach number focusing is particulary pronounced at expansion conditions were cooling sets in. Cluster formation in a supersonic jet takes place in the part of the expansion with the lowest temperature, which is on the jet axis. The lateral separation between the light and heavy components due to a different perpendicular velocity (temperature) is the consequence of this aggregation.

It is obvious from these observations that the correlation of mass and fluorescence spectra is affected by this effect.

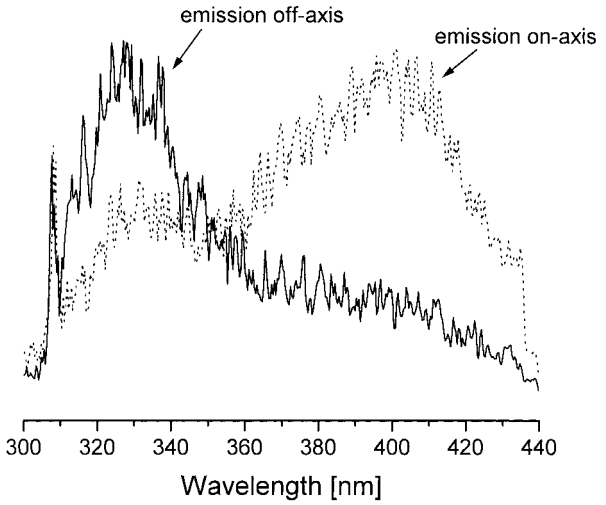

Figure 17. Emission spectra arising from the CCD image depicted in Figure 16. The spectra are averaged over different ranges on the CCD image [(−) emission from the outer part of the jet, (•••) emission arising from the inner core].

Although the TOF mass spectrometer analyzes only the on-axis particles passing the skimmer, the collection optics accepts fluorescence from a large solid angle. Therefore, the relative contributions of clusters and monomers in the mass and fluorescence spectra are different. To correlate both types of spectra one has to collect the fluorescence intensity emitted only near the beam axis. The intensity emitted from this region in the jet is depicted in Figure 17. The emission spectrum shows the largest contribution arising from the cluster emission. If the fluorescence intensity arising from the peripheral part of the jet is averaged, mostly monomer fluorescence is obtained in the spectrum (Figure 17).

Similar CCD images were observed for all investigated systems under the expansion conditions used here. We did not try to study this phenomenon systematically. But it appears to be a rather common phenomenon in a supersonic jet. In those cases where Mach number focusing was pronounced, the correlation between mass and fluorescence spectra was handled as already outlined.

Summary

R2PI and dispersed emission spectra of six jet-cooled bare and self-complexed DMABN derivatives were reported. The cluster size distribution was determined by TOF mass spectrometry and correlated with the excited species in the fluorescence experiment. Setting in with the formation of dimers in the supersonic expansion (for ABN at larger cluster sizes), a red-shifted emission band is observed. The red-shifted emission is attributed to excimer formation. It is concluded, that a TICT relaxation cannot account for the red-shifted fluorescence in a homogeneous jet expansion of DMABN. The supersonic jet experiments indicate that the occurrence of the red-shifted emission requires a specific cluster geometry.

Enrichment of the larger (heavier) clusters on the supersonic jet axis was shown optically by the two-dimensional detection of the fluorescence emission. The phenomenon of Mach number focusing requires that the spatial inhomogenity of the emitting molecules has to be taken into account when cluster size distributions are correlated with fluorescence spectra.

Acknowledgment. EIN was kindly provided by Prof. Dr. Rettig, Humboldt-University Berlin, Germany, and TMCA and OMCA by Dr. J. Herbich, Polish Academy of Science, Poland. We acknowledge fruitful discussions with Prof. Dr. Rettig, Dr. J. Herbich, and Prof. Z. R. Grabowski, Polish Academy of Science. U. L. thanks the Hermann Willkomm-Stiftung for financial support.

Registry No. DMABN, [1197-19-9]; ABN, [873-74-5]; DMABEE, [10287-53-3].

References and Notes

(1) Lippert, E.; Lüder, W.; Boos, H. In *Adv. Mol. Spectrosc. Proc. Int. Meet 4th 1959;* Mangini, A., Ed.; Pergamon: Oxford, 1962; p 443.
(2) For reviews see (a) Rettig, W. In *Topics in Current Chemistry, Vol. 169;* Mattay, J., Ed.; Springer: Berlin, 1994; p 254. (b) Serrano-Andres, L.; Merchan, M.; Roos, B. O.; Lindh, R. *J. Am. Chem. Soc.* **1995**, *117*, 3189. (c) Howell, R.; Phillips, D.; Hrvoje, P.; Keitaro, Y.; Petek, H.; Yoshihara, K. *Chem. Phys.* **1994**, *188*, 303. (d) Bhattacharyya, K.; Chowdhury, M. *Chem. Rev.* **1993**, *93*, 507.
(3) Schuddeboom, W.; Jonker, S. A.; Warman, J. M.; Leinhos, U.; Kühnle, W.; Zachariasse, K. A. *J. Phys. Chem.* **1992**, *96*, 10809.
(4) Rotkiewicz, K.; Grellmann, K. H.; Grabowski, Z. R. *Chem. Phys. Lett.* **1973**, *19*, 315.
(5) Visser, R. J.; Varma, C. A. G. O.; Konijnenberg, J.; Bergwerf, P. *J. Chem. Soc., Faraday Trans. 2* **1983**, *79*, 347.
(6) de Lange, M. C. C.; Leeson, D. T.; van Kuijk, K. A. B.; Huizer, A. H.; Varma, C. A. G. O. *Chem. Phys.* **1993**, *174*, 425.
(7) Chandross, E. A.; Thomas, H. T. *Chem. Phys. Lett.* **1971**, *9*, 397.
(8) Weisenborn, P. C. M.; Huizer, A. H.; Varma, C. A. G. O. *Chem. Phys*. **1989**, *133*, 437.
(9) Zachariasse, K. A.; von der Haar, T.; Hebecker, A.; Leinhos, U.; Kühnle, W. *Pure Appl. Chem.* **1993**, *65*, 1745.
(10) Zachariasse, K. A.; Grobys, M.; von der Haar, T.; Hebecker, A.; Il'ichev, Y. V.; Jiang, Y. B.; Morawski, O.; Kühnle, W. *J. Photochem. Photobiol. A. Chem.* **1996**, *102*, 59.
(11) Khalil, O. S. *Chem. Phys. Lett.* **1975**, *35*, 172.
(12) Khalil, O.; Hofeldt, R.; McGlynn, S. P. *J. Lumin.* **1973**, *6*, 229.
(13) Nakashima, N.; Mataga, N. *Bull. Chem. Soc. Jpn.* **1973**, *46*, 3016.
(14) Kato, S.; Amatatsu Y. *J. Chem. Phys.* **1990**, *92*, 7241.
(15) Majumdar, D.; Sen, R.; Bhattacharyya, K.; Bhattacharyya, S. P. *J. Phys. Chem*. **1991**, *95*, 4324.
(16) Sobolewski, A. L.; Domcke, W. *Chem. Phys. Lett.* **1996**, *259*, 119.
(17) Mordzinski, A.; Sobolewski, A. L.; Levy, D. H. *J. Phys. Chem. A* **1997**, *101*, 8221.
(18) Scholes, G. D.; Phillips, D.; Gould, I. R. *Chem. Phys. Lett.* **1997**, *266*, 521.
(19) Itoh, M.; Kajimoto O. In *Dynamics of excited molecules*; Kuchitsu, K., Ed.; Elsevier: Amsterdam, 1994.
(20) Wermuth, G.; Rettig, W. *J. Phys. Chem*. **1984**, *88*, 2729.
(21) Rettig, W.; Wermuth, G. *J. Photochem.* **1985**, *28*, 351.
(22) Sansonetti, C. J.; Salit, M. L.; Reader, J. *Appl. Opt.* **1996**, *35* , 74.
(23) Lahmann, C. Ph.D. Thesis, University of Frankfurt/M, Germany, April 1995.
(24) Rotkiewicz, K.; Grabowski, Z. R.; Krowczynski, A.; Kühnle, W. *J. Lumin.* **1976**, *12/13*, 877.
(25) Grassian, V. H.; Warren, J. A.; Bernstein, E. R.; Secor, H. V. *J. Chem. Phys.* **1989**, *90*, 3994.
(26) Gibson, E. M.; Jones, A. C.; Phillips, D. *Chem. Phys. Lett.* **1987**, *136*, 454.
(27) Kobayashi, T.; Futakami, M.; Kajimoto, O. *Chem. Phys. Lett.* **1986**, *130*, 63.
(28) Quan-yuan, S.; Bernstein, E. R. *J. Chem. Phys.* **1992**, *97*, 60.
(29) Varsany, G. *Assignments for vibrational spectra of seven hundred benzene derivatives*; Wiley: New York, 1974.
(30) Gibson, E. M.; Jones, A. C.; Phillips, D. *Chem. Phys. Lett.* **1988**, *146*, 270.
(31) Yu, H.; Joslin, E.; Crystall, B.; Smith, T.; Sinclair, W.; Phillips, D. *J. Phys. Chem.* **1993**, *97*, 8146.
(32) Herbich, J.; Salgado, F. P.; Rettschnick, R. P. H.; Grabowski, Z. R.; Wojtowicz, H. *J. Phys. Chem.* **1991**, *95*, 3491.
(33) Kobayashi, T.; Futakami, M.; Kajimoto, O. *Chem. Phys. Lett.* **1987**, *141*, 450.
(34) Ahlbrecht, H.; Düber, E. O.; Epsztajn, J.; Marcinkowski, R. M. K. *Tetrahedron* **1984**, *40*, 1157.
(35) A twist angle of ∼80° has been obtained in an ab initio geometry optimizations at the HF level of theory with a double-ζ basis set.
(36) Howell, R.; Jones, A. C.; Taylor, A. G.; Phillips, D. *Chem. Phys. Lett.* **1989**, *163*, 282.
(37) Peng, L. W.; Dantus, M.; Zewail, A. H.; Kemnitz, K.; Hicks, J. M.; Eisenthal, K. B. *J. Phys. Chem.* **1987**, *91*, 6162.
(38) Lommatzsch, U.; Brutschy, B. *Chem. Phys.* **1998**, *234*, 35.
(39) Guchhait, N.; Chakraborty, T.; Bera, P. K.; Nath, D.; Chowdhury, M. *J. Mol. Struct.* **1994**, *327*, 161.

(40) Hollas, J. M. *High-resolution spectroscopy*; Butterworth: London, 1982.
(41) Hassan, K. H.; Hollas, J. M. *J. Mol. Spec.* **1991**, *147*, 100.
(42) Petruska, J. *J. Chem. Phys.* **1961**, *34*, 1111.
(43) Wermuth, G. *Z. Naturforsch.* **1983**, *38a*, 368.
(44) Leinhos, U.; Kühnle, W.; Zachariasse, K. A. *J. Phys. Chem.* **1991**, *95*, 2013.
(45) Saigusa, H.; Itoh, M. *J. Phys. Chem.* **1985**, *89*, 5486.
(46) Lembach, G.; Brutschy, B. *J. Phys. Chem.* **1996**, *100*, 19758.
(47) (a) Meek, J. T.; Long, S. R.; Reilly, J. P. *J. Phys. Chem.* **1982**, *86*, 2809. (b) Walter, K.; Scherm, K.; Boesl, U. *J. Phys. Chem.* **1991**, *95*, 1188.
(48) Howell, R.; Petek, H.; Phillips, D.; Yoshihara, K. *Chem. Phys. Lett.* **1991**, *183* , 249.
(49) Phillips, D.; Howell, R.; Taylor, A. G. *Proc. Indian Acad. Sci. (Chem. Sci.)* **1992**, *104*, 153.
(50) Wersink, R. A.; Wallace, S. C. *J. Phys. Chem.* **1994**, *98*, 10710.
(51) Dedonder-Lardeux, C.; Jouvet, C.; Martrenchard, S.; Solgadi, D.; McCombie, J.; Howells, B. D.; Palmer, T. F.; Subaric-Leitis, A.; Monte, C.; Rettig, W.; Zimmermann, P. *Chem. Phys.* **1995**, *191*, 271.
(52) Kobayashi, T.; Honma, K.; Kajimoto, O.; Tsuchiya, S. *J. Chem. Phys.* **1987**, *86*, 1111.
(53) Heine, A.; Herbst-Irmer, R.; Stalke, D.; Kühnle, W.; Zachariasse, K. A. *Acta Crystallogr.* **1994**, *B50*, 363.
(54) Rühl, E. Ph.D. Thesis, University of Berlin (FU), Germany, May 1987.
(55) Revill, J. A. T.; Brown, R. G. *Chem. Phys. Lett.* **1992**, *188* , 433.
(56) Förster, T. *Pure Appl. Chem.* **1962**, *4*, 121.
(57) Rotkiewicz, K.; Leismann, H.; Rettig, W. *J. Photochem. Photobiol. A Chem.* **1989**, *49*, 347.
(58) Birks, J. B. *Photophysics of aromatic molecules;* Wiley: New York, 1970.
(59) Yip, W. T.; Levy, D. H. *J. Phys. Chem.* **1996**, *100*, 11539.
(60) Saigusa, H.; Lim, E. C. *Acc. Chem. Res.* **1996**, *29*, 171.
(61) The exciton resonance interaction is calculated using eq 2 and assuming an intermolecular distance of 3.5 Å. The transition dipole moment M is given by $f_{state} = 4.2 \times 10^{52}\ C^{-2}m^{-2}cm\ \bar{\nu}|M|^2$ with the oscillator strength f and the energy $\bar{\nu}$ of the transition into the L_a, L_b state, respectively. The oscillator strengths according to ref 2b are $f(L_b) = 0.005$ and $f(L_a) = 0.510$, and the difference in excited-state energies of the L_b and L_a states is 0.19 eV. For the energy of the L_b state, the experimental energy for the electronic origin of the monomer of 4 eV is employed.
(62) (a) Rettig, W.; Dedonder-Lardeux, C.; Jouvet, C.; Martrenchard-Barra, S.; Szrifiger, P.; Krim, L.; Castano, F. *J. Chim. Phys.* **1995**, *92*, 465. (b) Zlatkis, A.; Lee, C. K.; Wentworth, W. E.; Chen, E. C. M. *Anal. Chem.* **1983**, *55*, 1596.
(63) Brenner, V.; Millie, Ph.; Piuzzi, F.; Tramer, A. *J. Chem. Soc., Faraday Trans.* **1997**, *93*, 3277.
(64) Haas, Y.; Anner, O. In *Photoinduced Electron Transfer, Part A*; Fox, A. M.; Chanon, M., Eds.; Elsevier: Amsterdam, 1988.
(65) Saigusa, H.; Sun, S.; Lim, E. C. *J. Phys. Chem.* **1992**, *96*, 2083.
(66) Sharma, P. K.; Knuth, E. L.; Young, W. S. *J. Chem. Phys.* **1976**, *64*, 4345.
(67) DePaul, S.; Pullman, D.; Friedrich, B. *J. Phys. Chem.* **1993**, *97*, 2167.
(68) Becker, E. W.; Bier, K.; Burghoff, H. *Zeit. Naturforsch.* **1955**, *10a*, 565.
(69) Waterman, P. C.; Stern, S. A. *J. Chem. Phys.* **1959**, *31*, 405.
(70) Miller, R. In *Atomic and Molecular Beam Methods, Vol. 1*; Scoles, G., Ed.; Oxford University: New York, 1988.
(71) Becker, E. W.; Beyrich, W.; Bier, K.; Burghoff, H.; Zigan, F. *Zeit. Naturforsch.* **1957**, *12a*, 609.
(72) Malakhovskii, A.; Gedanken, A. *Chem. Phys.* **1997**, *221*, 215.
(73) Malakhovskii, A.; Gedanken, A. *J. Chem. Soc., Faraday Trans.* **1997**, *93*, 3005.
(74) Schmidt, A. Diploma Thesis, University of Frankfurt/M, Germany, October 1995.